Miscibility, Interactions and Antimicrobial Activity of Poly(ε-caprolactone)/Chloramphenicol Blends

Eva Sanchez-Rexach[1*], Emilio Meaurio[1], Jagoba Iturri[2], José L. Toca-Herrera[2], Sivan Nir[3], Meital Reches[3*], Jose-Ramon Sarasua[1]

[1]Department of Mining-Metallurgy Engineering and Materials Science, POLYMAT, School of Engineering, University of The Basque Country (UPV/EHU), Alameda Urquijo s/n, Bilbao, Spain.

[2] Department of Nanobiotechnology, Institute for Biophysics, University of Natural Resources and Life Sciences (BOKU), Muthgasse 11, Vienna 1190, Austria

[3]Institute of Chemistry, The Hebrew University of Jerusalem, Edmond J Safra Campus, IL-9190401 Jerusalem, Israel

* Corresponding authors: evagloria.sanchez@ehu.eus (E. Sanchez-Rexach)
meital.reches@mail.huji.ac.il (Reches, Meital)

Abstract

Poly(ε-caprolactone) (PCL) has been blended with Chloramphenicol (CAM), a well-known bacteriostatic antibiotic, in order to obtain new biomaterials with antibacterial properties. The resulting samples have been thoroughly characterized regarding both their physicochemical behavior and antimicrobial efficacy by means of very diverse techniques. Hence, PCL/CAM blend miscibility has been analyzed by Differential Scanning Calorimetry (DSC) using the single glass transition temperature (T_g) criterion, intermediate between those corresponding to the two components in the blend. In turn, the interaction parameter has been obtained from the analysis of the melting point depression in both PCL-rich and CAM-rich blends. Fourier-Transform Infra-Red (FTIR) spectroscopy and X-Ray Diffraction (XRD) analysis have been used -in the pure components and in the blends- to analyze both the specific interactions and the crystallization behavior, respectively. The morphology of PCL/CAM blends obtained by spin-coating has been also studied by means of Atomic Force Microscopy (AFM). Finally, drug release kinetics of different PCL/CAM systems as well as their antibacterial efficacy against *Escherichia Coli* have been investigated, indicating that CAM can be released from the PCL/CAM blends in a controlled way while keeping intact the antibacterial efficiency.

Keywords: poly(ε-caprolactone) (PCL); chloramphenicol (CAM); miscibility; interactions; spherulitic morphology; release kinetics; antibacterial performance.

1. Introduction

A controlled drug-delivery device is that able to deliver the drug at the desired release rate and duration, thus maintaining the drug level in the body within the therapeutic window (see Sch. 1). Upon intake, drug molecules must be dissolved in aqueous-based gastrointestinal fluids in a sufficient quantity as to reach their whatsoever therapeutic effect. Nevertheless, most drugs are in crystalline form, which implies auto-association interactions and low water solubility [1]. A successful strategy to improve the solubility of poorly soluble drugs is to dispense the drug in the form of amorphous solid dispersions (ASDs).

The dispersion of a drug into a polymeric matrix enables the establishment of strong specific interactions with its functional groups, provided that they have complementary interacting groups. Thus, the chemical potential of the drug in the amorphous phase is reduced, and as a result, its crystallization can be hindered. In other words, miscibility between the two components should favor the formation of ASDs, preventing the crystallization of the drug, and as a result, enhancing its solubility [2]. The drug release mechanism from a polymer depends on parameters such as the nature of the polymer, matrix geometry, drug-related properties, initial drug loading, and drug-matrix interactions [3]. If, in addition, a medical device is made of a biodegradable polymer, it does not have to be removed after finishing its task. Furthermore, in a biodegradable polymer-drug system the control of the degradation rate of the biodegradable polymer enables the control of the drug release from the matrix [4].

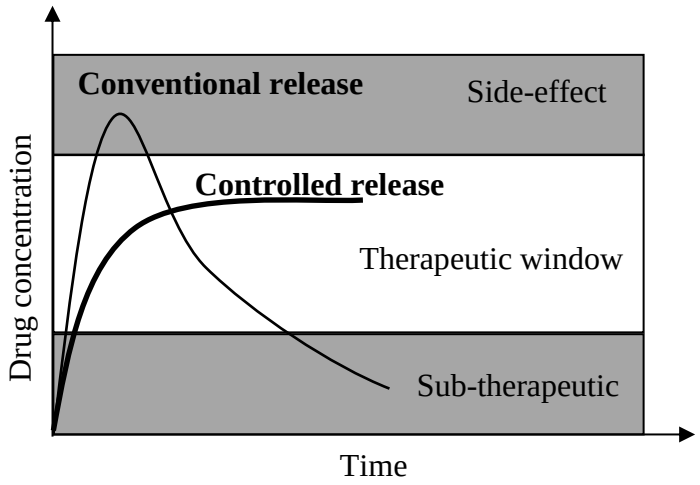

Scheme 1. A comparison of conventional drug delivery profile vs. a controlled drug release profile.

In this regard, Poly(ε-caprolactone) (PCL) is one of the most promising biodegradable polymers and is already widely used in biomedical applications. PCL is suitable for long-term biomedical applications since its degradation can last from several months to years [5]. In turn, Chloramphenicol (CAM) is a broad-spectrum bacteriostatic antibiotic, which diffuses through the bacterial cell and binds to 50S ribosomal subunit. Such interaction induces the inhibition of the bacterial protein synthesis as well as the blocking of bacterial cell proliferation. A wide range of microorganisms can be effectively treated by CAM [6]; for example, it is useful in the treatment of staphylococcal brain abscesses due to an excellent blood-barrier penetration or meningitis caused by *Enterococcus faecium*. Its employment has also been shown to be effective in treating ocular infections caused by a number of bacteria including *Staphylococcus aureus*, *Streptococcus pneumoniae* and *Escherichia coli* [7]. As main disadvantage CAM shows low aqueous solubility [8].

Considering the respective chemical structures of the two species under study (see Sch. 2), hydrogen bonding can be expected to be formed between the hydroxyl groups of CAM and the carbonyl groups of PCL. In this paper, the miscibility of the PCL/CAM blends is analyzed using the criterion of the single intermediate glass transition temperature (T_g), while the strength of the resulting intermolecular interactions is evaluated from the interaction parameter. FTIR spectroscopy is then used to analyze the specific interactions responsible for the miscibility of the blends. Moreover, morphological changes in the blends are discussed in terms of PCL/CAM intermolecular interactions through the analysis of the spherulitic growth by means of AFM. The suitability of the blends for biomedical applications has been analyzed by investigating the release kinetics of CAM in PBS solution at 37 ºC, as well as by analyzing the antibacterial efficacy of the PCL/CAM blends against *Escherichia Coli* conducting the agar diffusion test. *E. Coli* is a gram-negative etiologic agent associated with biofilm formation on implants and susceptible to chloramphenicol treatment. The results obtained by these techniques show that CAM can be released in a controlled way from the PCL/CAM blends.

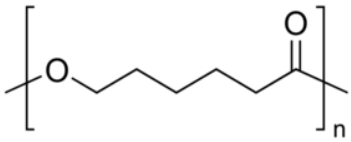

Poly(ε-caprolactone)

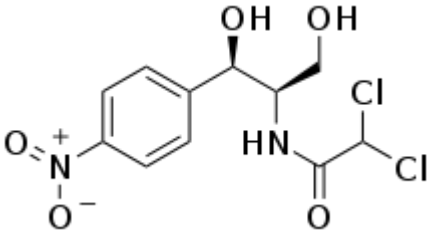

Chloramphenicol

Scheme 2. Chemical structures of PCL and CAM.

2. Experimental Section

2.1. Starting Materials

Poly(ε-caprolactone) (PURASORB® PC12 trade name) with an average molecular weight (M_w) of $1.3 \cdot 10^5$ g mol^{-1} and $M_w/M_n = 1.76$ (as determined by GPC) was obtained from Purac Biochem (The Netherlands). Chloramphenicol (purity ≥ 98 %) and Phosphate Buffered Saline (PBS) solution 1 M (pH 7.4) were supplied by Aldrich Chemical Cor (Spain). *Escherichia coli* (ATCC 1655) was purchased from ATCC (Virginia, USA).

2.2 Blend Preparation

Films were prepared by casting from tetrahydrofuran (THF) solutions at room temperature. Films 100 μm thick were prepared by casting from 2.7 wt% solutions into 60 mm diameter Petri dishes, and films 800 nm thick were obtained by spin-coating onto glass substrates from 10 mg/mL solutions using a spin-coater (Schaefer Tech) operating at 1000 rpm for 60 s.

2.3. Differential Scanning Calorimetry (DSC)

Thermal analyses were conducted on a Modulated DSC Q200 from TA Instruments. All the scans were carried out in hermetic aluminum pans under nitrogen atmosphere with sample weights between 5 and 10 mg. In order to study the glass transition temperatures, two consecutive scans were performed from -80 ºC to 180 ºC with a scan rate of 20 ºC/min, ensuring complete melting of the sample. Glass transition temperatures (T_g) were measured in the second scan as the midpoint of the specific heat increment.

2.4. Melting Point Depression

The melting point depression of CAM was investigated from CAM-rich blends containing 100-70 wt% CAM. Samples were heated in the DSC with a scan rate of

1 ºC/min to obtain the melting temperature of the CAM crystals. No weight loss was observed during the thermal treatments.

The melting point depression of PCL was analyzed from PCL/CAM blends containing 100-80 wt% PCL. Samples were first heated at 180 ºC for 3 min to assure complete melting of the PCL and CAM crystals, and then cooled at 10 ºC/min to the desired crystallization temperatures (T_c) allowing to crystallize isothermally for 60 min. Then, they were heated to 180ºC to obtain the melting points with a scan rate of 10 ºC/min.

2.5. Fourier Transform Infrared Spectroscopy (FTIR)

FTIR spectra were recorded on a Nicolet AVATAR 370 Fourier transform infrared spectrophotometer. Spectra were taken with a resolution of 2 cm^{-1} and were averaged over 64 scans in the 4000-450 cm^{-1} range. Tetrahydrofuran solutions (1.1 wt%) were cast on KBr pellets by evaporation of the solvent at room temperature. Traces of tetrahydrofuran were removed placing the films into a heated vacuum oven for 24 h. The absorbance of the samples was within the range where the Lambert-Beer law is obeyed. A controlled high temperature transmission cell mounted in the spectrometer was used to obtain the spectra of molten samples. Second derivative spectra were smoothed using the Norris-Williams Gap Derivatives [9] using maximum gap sizes and segment lengths of 5 points and 5 cm^{-1} respectively in the derivative transformations.

2.6. X-ray Diffraction (XRD)

X-ray powder diffraction patterns were collected by using a Philips X'pert PRO automatic diffractometer operating at 40 kV and 40 mA, in theta-theta configuration, secondary monochromator with Cu-Kα radiation (λ = 1.5418 Å) and a PIXcel solid state detector (active length in 2θ 3.347º). Data were collected from 5 to 50° 2θ (step size 0.026 and time per step = 700 s) at room temperature. A fixed divergence and antiscattering slit giving a constant volume of sample illumination was used.

2.7. Atomic Force Spectroscopy (AFM)

An AFM instrument Nanowizard I (JPK Instruments, Germany) was operated in air, using contact imaging mode at constant loading forces and rates. Cantilevers were calibrated before each experiment by means of the thermal tune method [10]. Silicon-nitride probes (DNP-10, Bruker, USA) with a nominal spring constant of 0.12 N/m were used in the experiments. All images were processed using the JPK data analysis software.

2.8. In Vitro Release Studies and Release Kinetics (UV-Vis)

UV–Vis absorption spectra were recorded over wavelengths ranging from 190 to 500 nm using a Perkin Elmer Lamda 265 UV-Visible spectrophotometer. Before

performing the drug release experiments, a calibration curve was obtained measuring the absorbance at a wavelength of 278 nm for solutions of chloramphenicol in 0.1 M PBS (pH 7.4) with concentrations ranging from 10 to 100 ppm. Square samples of PCL/CAM films of 1 cm^2 with a thickness of 100 μm obtained by solvent casting were immersed in 100 mL of 0.1 M PBS buffer at 37 ºC. At fixed time intervals, samples of 2 mL were taken and replaced with fresh PBS at 37 ºC. Drug concentration in solution was determined by UV spectroscopy using the calibration curve.

The release kinetics of chloramphenicol were examined considering three mathematical models [11, 12, 13]:

1. Zero order: $C_t/C_\infty = k_0 t$ (1)
2. First order: $\ln (1- C_t/C_\infty) = -k_1 t$ (2)
3. Higuchi: $C_t/C_\infty = k_h t^{1/2}$ (3)

C_t is the cumulative amount of drug released at time *t*, C_∞ represents the starting amount of drug; and k_0, k_1 and k_h are constants.

2.9. Agar Diffusion Test (*E. coli*)

Square samples (1 cm^2) of PCL/CAM 50/50 and 80/20 blends obtained by solvent casting were tested for antibacterial activity. The films were placed in 3 mL PBS buffer at 37 ºC and 5 μl of the solution were taken at fixed intervals (30 min, 3 h and 24 h), and poured over Luria-Bertani (LB) agar plates containing *E.Coli*. As positive control, drops of pure chloramphenicol (1 mg/mL) were placed in the same manner on the plates. A negative control was also examined in the form of PCL film, in order to demonstrate that the PCL does not have antibacterial traits. Radius of inhibition zones were measured to evaluate the antibacterial efficacy.

3. Results and Discussion

3.1. PCL/CAM Blend Characterization

3.1.1. DSC Analysis of Thermal Transitions and Miscibility

When two polymeric materials are miscible, macroscopic properties of single-phase materials are expected for the blend, such as a single glass transition temperature intermediate between those of the pure components [14, 15, 16]. This intermediate T_g usually obeys the Fox equation [17]:

$$\frac{1}{T_{gb}} = \frac{w_1}{T_{g1}} + \frac{w_2}{T_{g2}} \quad (4)$$

where w_1 and w_2 are the weight fractions of components 1 and 2 respectively, T_{g1} and T_{g2} are the glass transition temperatures of the pure components, and T_{gb} is the glass transition temperature of the blend (values in Kelvin).

It can be observed that PCL is a semicrystalline polymer melting at about 66 ºC, while CAM is a crystalline solid melting at about 153 ºC (see Table 1). In addition, all the PCL/CAM blends display the two melting endotherms corresponding to the pure components of the blend in the crystalline state (see Figure S1 of the Supporting Information). Figure 1 shows the second scan DSC curves recorded after cooling from the melt (cooling rate ~20 ºC/min) for PCL, CAM and their blends. As can be seen, fast cooled CAM results in a super cooled liquid which shows the glass transition temperature at about 32 ºC. The glass transition temperature of PCL is located at about -60 ºC. Below the T_g of CAM, molecular mobility is frozen, nucleation points are no longer formed and crystallization of the drug is inhibited [18]. Supercooling also enhances the glass transition temperature jumps observed in the second scan for the PCL/CAM blends, which show single T_gs intermediate between those of the pure components in the whole composition range. Consequently, the two components are completely miscible in the amorphous phase. As shown in Table 1, the observed T_gs are close to the values predicted by the Fox equation (Eq. 4). It should be noted that second DSC traces for PCL/CAM 60/40 and 50/50 blends present an exothermic peak between T_g and T_m (see Fig. 1), corresponding to the crystallization of the PCL (see Table 1). Furthermore, as can be seen in Fig. 1, there is a slight broadening of the T_g due to the compositional heterogeneity representative of miscible systems.

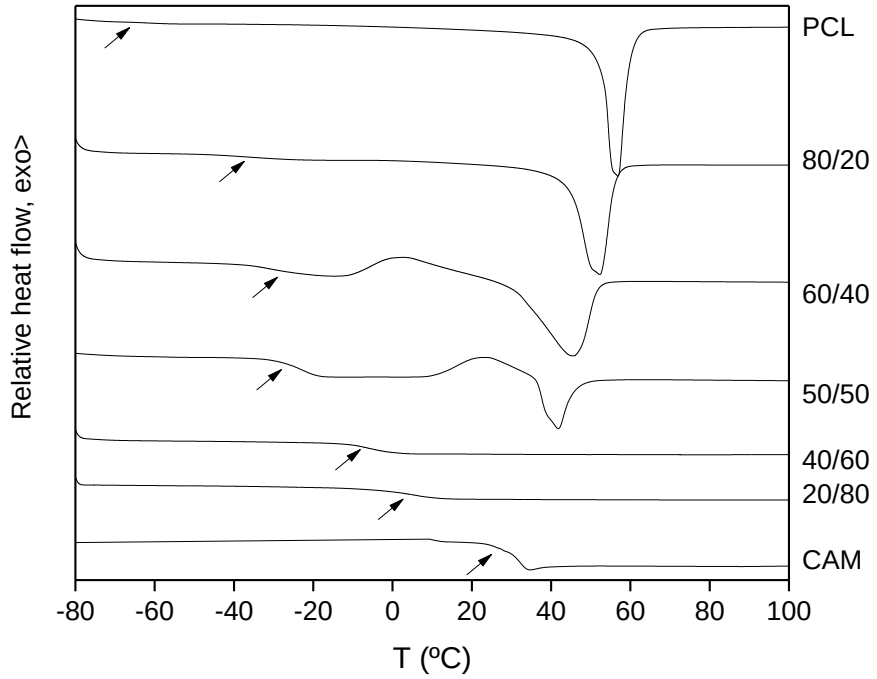

Figure 1. Second scan DSC traces for PCL, CAM and PCL/CAM blends.

Table 1. Thermal properties of PCL/CAM blends.

	First Scan				Second Scan					
PCL/CAM	T_m PCL ºC	ΔH_m PCL J/g	T_m CAM ºC	ΔH_m CAM J/g	T_g experimental ºC	T_g calculated ºC	T_c PCL ºC	ΔH_c PCL J/g	T_m PCL ºC	ΔH_m PCL J/g
PCL	66.5	81.6	-	-	-60	-	-	-	57.2	66.4
80/20	60.1	66.8	109.8	9.7	-36	-46	-	-	52.3	58.1
60/40	60.2	58.8	136.9	26.9	-32	-31	3.4	21.5	45.7	35.0
50/50	62.2	45.7	142.1	42.8	-21	-22	23.4	7.1	41.5	9.1
40/60	57.6	30.3	148.5	68.8	-7	-13	-	-	-	-
20/80	60	22.3	150.7	70.4	6	8	-	-	-	-
CAM	-	-	152.9	136.4	32	-	-	-	-	-

3.1.2. Melting Point Depression Analysis

The free energy of mixing of a polymer-drug binary system is described by the Flory-Huggins solution theory [19, 20]. Thermodynamically, the change in free energy at the melting point is zero ($\Delta G = \Delta H - T_m\Delta S = 0$), hence $T_m = \Delta H/\Delta S$, and since the entropy change in a miscible blend (entropy of melting plus entropy of mixing) is larger than in the pure component, the melting temperature decreases [19, 21]. The depression of the equilibrium melting point can be analyzed using Flory's relationship [20]:

$$\frac{1}{T_{me}} - \frac{1}{T_{me}^{0}} = \frac{-R}{\Delta H_{2u}} \frac{V_{2u}}{V_{1u}} \left(\frac{\ln \phi_2}{m_2} + \left(\frac{1}{m_2} - \frac{1}{m_1} \right) \phi_1 + \chi_{12} \phi_1^2 \right) \qquad (5)$$

where T_{me}^{0} and T_{me} are, respectively, the equilibrium melting points of the pure crystallizable component and of its blends, the subscripts *1* and *2* refer to the amorphous and crystallizable components respectively, R is the universal gas constant, ΔH_u is the heat of fusion per mole of crystalline repeat units, V_u is the molar volume of the repeating unit, m is the degree of polymerization, ϕ is the volume fraction, and χ_{12} is the polymer-polymer interaction parameter.

To apply Eq. (5) to the analysis of the melting point depression of CAM (component 2), the molar volume of liquid CAM (V_2 = 220 cm^3/mol [22]) is taken as the molar volume of the lattice sites, and consequently $m_2 = 1$. In addition, the same volume can be adopted as the molar volume of the polymeric repeat unit ($V_2 = V_{1u}$) so that $1/m_1 \approx 0$ (since $m_1 = V_1/V_{1u}$ is large). Therefore, Eq. (5) simplifies to Eq. (6):

$$\frac{1}{T_m} - \frac{1}{T_m^{0}} = \frac{-R}{\Delta H_2} \left(\ln \phi_2 + \phi_1 + \chi \phi_1^2 \right) \qquad (6)$$

The melting point of CAM has been measured at low heating rates (1 ºC/min) for the pure component and for different PCL/CAM blends (see Table 2). The average melting point of pure Chloramphenicol is T_mº(CAM) = 150.8 ºC, and the addition of 30 wt% PCL decreases the melting point by about 6 ºC. Using the average melting enthalpy of pure CAM (ΔH_{CAM} = 119 J/g), the data in table 2 have been analyzed according to Eq. (6) yielding the plot in Figure 2a. The negative value obtained for χ (-0.2) confirms a thermodynamically miscible blend. Alternatively, the interaction energy density, B can be calculated at the melting temperature of CAM according to Eq. (7):

$$\chi = \frac{BV_r}{RT} \tag{7}$$

where V_r is a reference volume (in this case, $V_r = V_2 = 220$ cm^3/mol), yielding B = - 3 J/cm^3.

Table 2. Melting temperature of CAM in CAM-rich PCL/CAM blends.

CAM wt%	T_m (ºC)		
	Sample 1	Sample 2	Sample 3
100	150.8	150.8	150.8
90	149.3	149.3	149.3
80	147.9	147.4	147.6
70	145.5	145.2	145.3

When equation 5 is applied to the melting point depression of a polymer (m_2 >> 1) in a polymer-drug system, the molar volume of the amorphous drug is usually adopted as the molar volume of the lattice cells ($m_1 = 1$), leading to:

$$\frac{1}{T_{me}} - \frac{1}{T_{me}^0} = \frac{-R}{\Delta H_{2u}} \frac{V_{2u}}{V_1} \left(-\phi_1 + \chi \phi_1^2 \right) \tag{8}$$

Nevertheless, in case of polymers, morphological effects such as lamellae thinning due to the penetration of the amorphous blend partner in the interlamellar region also contribute to the observed melting point depression, and must be accounted for [23]. The usual correction is the Hoffman-Weeks (H-W) method, which allows the determination of the equilibrium melting temperature of PCL in the pure polymer and in the blends [24] (see experimental). This method assumes a linear relation between the crystallization (T_c) and melting temperatures (T_m), and T_{me} is obtained from the intersection of this line with the $T_m = T_c$ line. Figure S2 of the Supporting Information displays the H-W plots to obtain the equilibrium melting temperatures for pure PCL (T_{me}^0) and blended PCL (T_{me}), which are summarized in Table 3. The decrease in the equilibrium melting temperatures suggests the miscibility of the system.

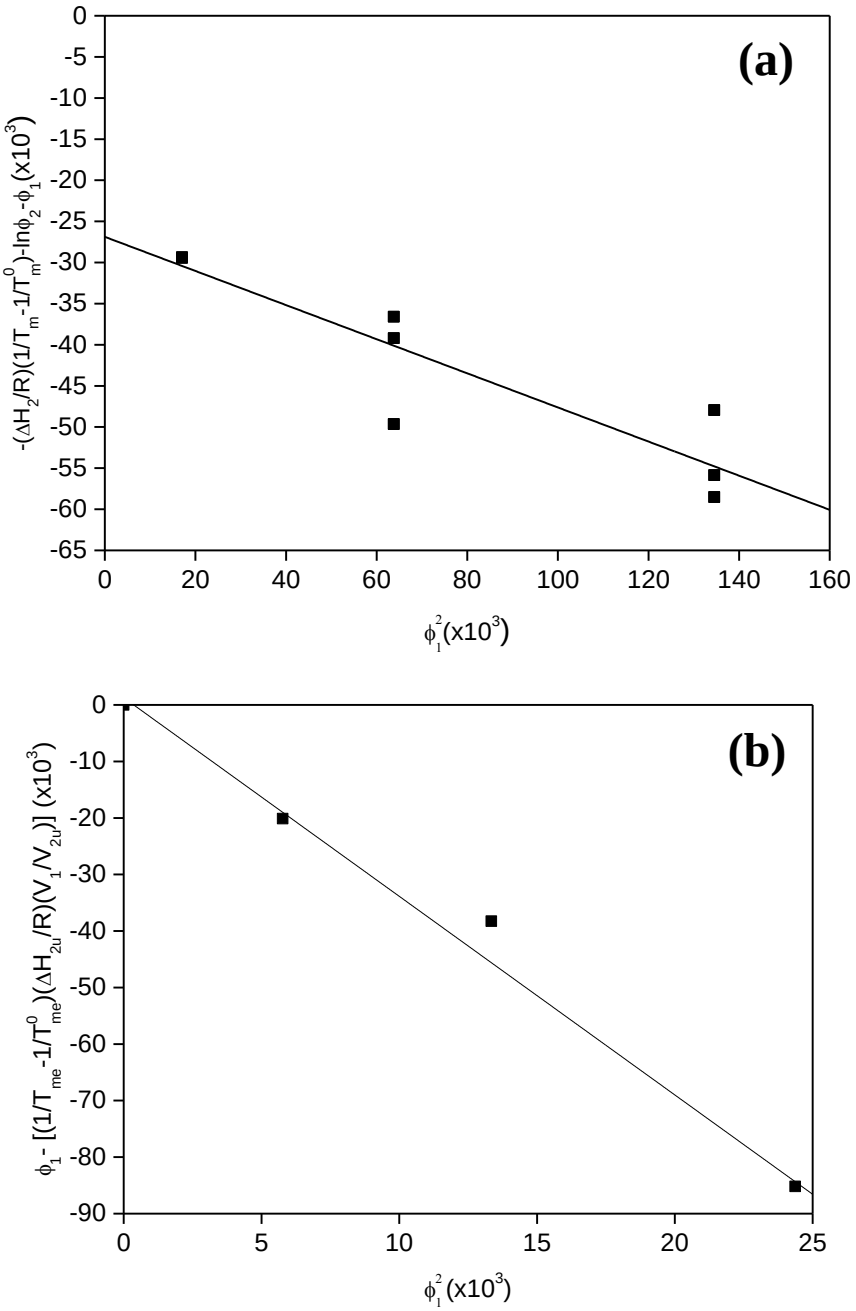

Figure 2. (a) Analysis of the melting temperature of CAM according to Eq. (6) in the presence of PCL. The slope of the plot gives the interaction parameter χ = -0.2; (b) Plot used to calculate the interaction parameter for the PCL/CAM system according to Eq. (8). The slope of the plot gives the interaction parameter χ = -3.4.

Table 3. Equilibrium melting temperatures (T_{me}) obtained from the H-W extrapolations.

System	T_{me} (ºC)
PCL	64.7
PCL/CAM 90/10	62.0
PCL/CAM 85/15	60.4
PCL/CAM 80/20	58.0

Figure 2b shows the analysis of the equilibrium melting temperatures according to the Flory-Huggins equation (Eq. 8). The parameters used in the calculations are V_1 = 220 cm^3/mol (CAM) [24], V_{2u} = 105 cm^3/mol and ΔH_{2u} = 140 J/g (PCL) [25]. From the slope the value obtained for the interaction parameter is χ = -3.4. The negative value obtained for χ confirms a thermodynamically miscible blend.

3.1.3. FTIR Analysis of PCL/CAM Blends

Figure 3a shows the X-H stretching region for molten CAM and PCL/CAM blends of different composition at 160 ºC. Pure CAM presents a peak at about 3400 cm^{-1} attributable to the N-H stretching mode of secondary amides participating in weak contacts [26, 27]. The O-H stretching band is the broad envelope from about 3200 to 3650 cm^{-1}, indicating a broad range of interaction strengths resulting from the adoption of the distorted hydrogen bonding geometries allowing interactions with the disordered amorphous environment [26]. In pure CAM, the maximum of the OH stretching band overlaps with the N-H stretching band, and occurs somewhere about 3450 cm^{-1}. Upon the addition of PCL to CAM, the OH stretching band shifts to higher wavenumbers, up to about 3500 cm^{-1} in the PCL-rich blends. The shift to higher wavenumbers is typical of systems in which the stronger OH···OH interactions are replaced by weaker C=O···O-H interactions, and suggests the establishment of intermolecular C=O···H-O interactions at the expense of the O-H···O-H autoassociation. Notice that the PCL/CAM 40/60 blend contains approximately equimolecular amounts of PCL repeat units and CAM molecules, and therefore contains approximately equimolecular amounts of C=O and OH groups.

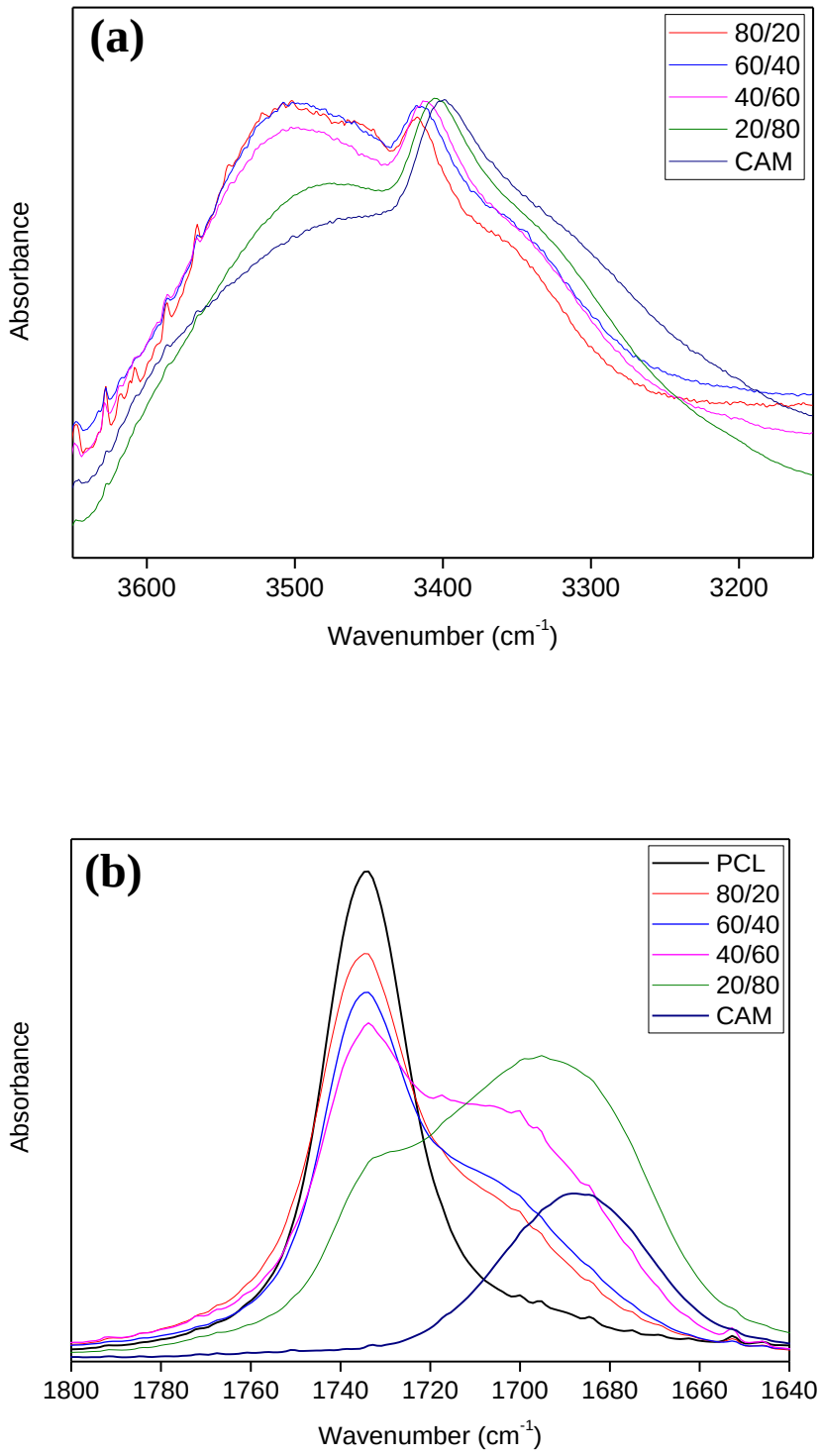

Figure 3. (a) X-H stretching region for the PCL/CAM system at 160 ºC; (b) Carbonyl stretching region for the PCL and PCL/CAM blends at 160 ºC

Figure 3b shows the carbonyl stretching region of the pure components and their blends in the melt (at 160 ºC). Molten PCL shows a peak at 1735 cm^{-1} attributable to free C=O groups in the amorphous phase and molten CAM shows a broad peak located at about 1688 cm^{-1} attributable to C=O groups hydrogen bonded to the hydroxyl groups present in pure CAM. As can be observed, blending results in a new band corresponding to the PCL associated with CAM that absorbs at lower wavenumbers than pure PCL, and is actually located between the bands of the pure components. However, the substantial overlap between the bands corresponding to the pure components makes difficult the identification of new bands in this spectral region. In order to improve spectral resolution, Norris second derivatives have been obtained for CAM and for the PCL/CAM 40/60 blend (see Fig. S3 of the supporting information) in both molten (160 ºC) and supercooled samples (40 ºC). The second derivative of supercooled CAM shows two components located at about 1690 and 1675 cm^{-1}, attributable to the two main conformers occurring in molten CAM, which only differ in the orientation of the terminal dichloromethyl group [26]. At 160 ºC, the second derivative spectrum of the PCL/CAM blend shows a new intermediate band located between those corresponding to free C=O groups of PCL and the hydrogen bonded C=O groups of CAM, that can be attributed to C=O groups of PCL hydrogen bonded to hydroxyl groups of CAM. After quenching to room temperature, the locations obtained for the two PCL bands using second derivative spectroscopy are respectively 1735 and 1709 cm^{-1}. The red shift obtained for the hydrogen bonded C=O groups of PCL is therefore 24 cm^{-1}. The analysis of the C=O stretching band confirms the occurrence of C=O···H-O hydrogen bonding between PCL and CAM.

3.1.4. Crystallization Behavior Based on the X-ray Diffraction Analysis

The XRD patterns of PCL, CAM and their blends are shown in Figure 4. CAM exhibits a characteristic peak at $2\theta = 13^{o}$, as well as several strong peaks at 16^{o}, 18^{o}, 19^{o} and 20^{o}. As the polymer content in the blend increases, the intensity of the crystalline peaks decreases while their width increases. The width of X-ray diffraction peaks is related to the size of the crystallites, and peak widening is usually a consequence of smaller, more imperfect crystals [28]. The PCL/CAM 90/10 blend still shows tiny CAM peaks, while in the PCL/CAM 95/5 blend crystallization of CAM is completely suppressed. Hence, completely amorphous CAM (as required in amorphous solid dispersions, ASDs) can only be obtained when the CAM content is below 10 wt%.

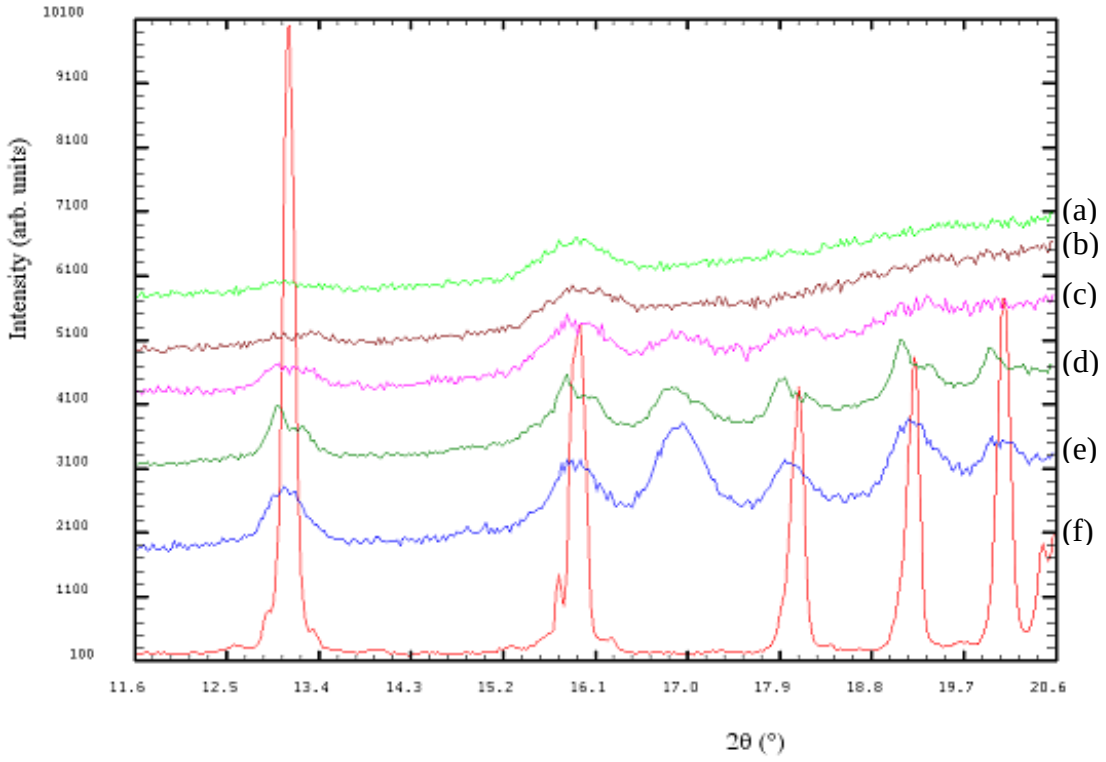

Figure 4. XRD patterns of: (a) pure PCL; (b) PCL/CAM 95/5; (c) PCL/CAM 90/10; (d) PCL/CAM 85/15; (e) PCL/CAM 80/20; and (f) pure CAM.

3.1.5. AFM Analysis

AFM topographic images of thin films (800 nm) of pure PCL, show the characteristic spherulitic morphology of semicrystalline polymers (Figure 5a). In the melt, PCL and CAM form a single phase, however, crystallization of PCL upon cooling creates a CAM enriched amorphous phase that is displaced by the growing crystalline phase to the interlamellar region and to the spherulitic grain boundaries [29]. As the CAM content in the blend increases, spherulitic boundaries become less defined, and the crystalline phase shows a looser, less compact morphology. The PCL/CAM 40/60 blend (Figure 5d) is a clear example of this behavior. In the PCL/CAM 20/80 blend (Figure 5e) crystallization of PCL is completely suppressed. Finally, Figure 5f shows the morphology observed in an immiscible PCL/drug blend (with erythromycin), characterized by straight interspherulitic boundaries similar to those observed in pure PCL samples.

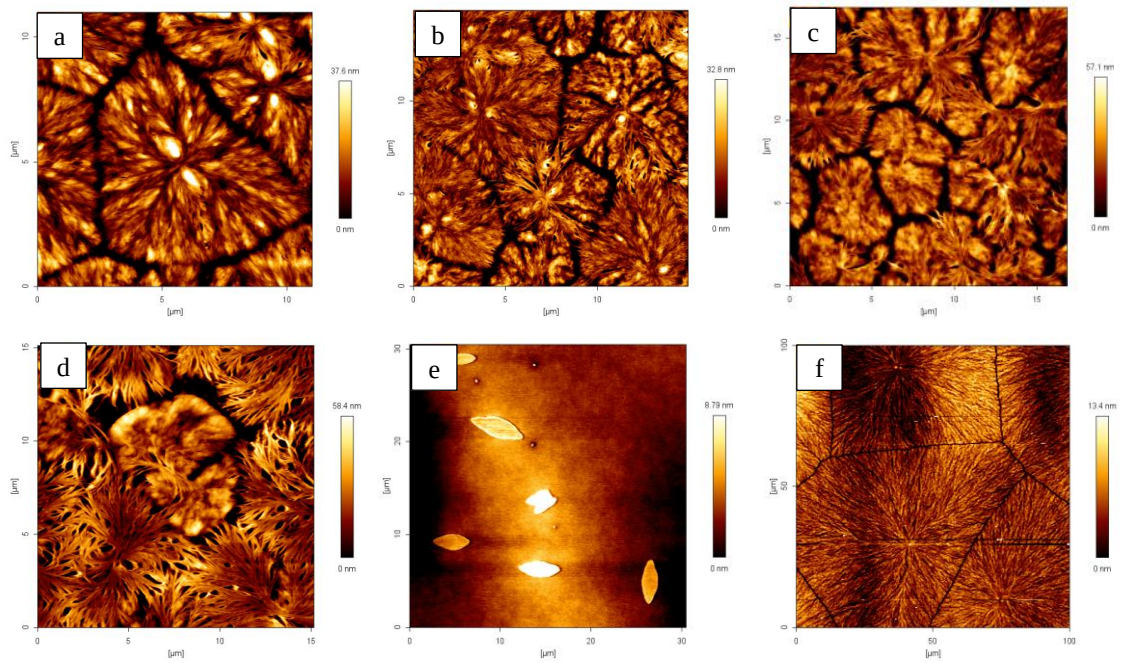

Figure 5. AFM topographic images: (a) pure PCL; (b) PCL/CAM 80/20; (c) PCL/CAM 60/40; (d) PCL/CAM 40/60; (e) PCL/CAM 20/80; and (f) PCL/Erythromycin 50/50 (immiscible). Films thicknesses were about 800 nm.

3.2. Drug Release Behavior

Figure 6 shows the in vitro drug release experiments performed for PCL/CAM 40/60, 80/20 and 95/5 blends for 7 hours (since the whole antibiotic was released within that time). Considering the release profiles of chloramphenicol coupled with the XRD results, two different release behaviors can be distinguished: one for PCL/CAM 40/60 and 80/20 blends, where part of the antibiotic is crystalline; and another one for PCL/CAM 95/5 blend, where the drug is in amorphous form. In the latter case, there is an initial burst in which 39 wt% of the drug is released during the first 10 minutes, whereas for the other two compositions only 5 wt% is released in the same period of time.

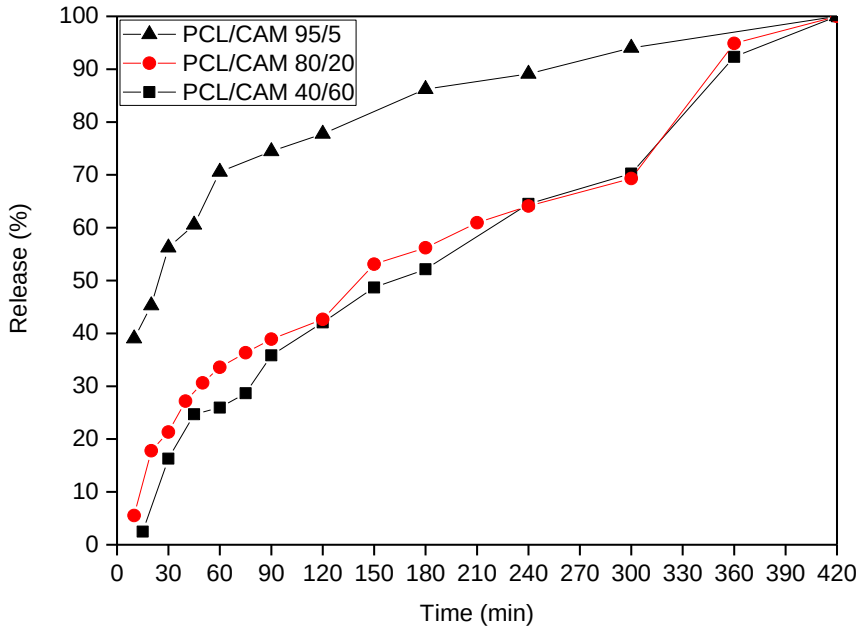

Figure 6. Drug release profile of PCL/CAM 40/60, 80/20 and 95/5 samples of 1 cm^2 with a thickness of 100 μm obtained by solvent casting, immersed into 100 mL of PBS (pH 7.4) at 37ºC for 7 hours.

The release process starts with the penetration of the buffered solution into the polymeric matrix leading to its swelling. Consequently, the free volume of the polymeric chains increases and the polymeric network becomes looser, leading to the diffusion of the amorphous chloramphenicol through the PCL matrix into the outer solution [30]. The release data has been fitted to different kinetic equations used to study the mechanism of drug release. Regression coefficients are shown in Table 4. PCL/CAM 95/5 system follows a first order kinetics, thus, the release depends on drug concentration. There is an initial burst, because the drug is in amorphous form and then, it is released in a controlled way. Therefore, it can be a good choice in applications where it is necessary to attain rapidly the effective therapeutic concentration and to maintain it for some hours.

On the other hand, the release from PCL/CAM 80/20 and 40/60 systems fits to zero order kinetics, where the release occurs at a constant rate, independent of the drug concentration used to prepare the blend. In the zero order kinetics, the CAM crystallites act as drug reservoirs that, after the initial burst, maintain the concentration of amorphous drug dissolved in the polymeric matrix in nearly steady conditions. This release mechanism is useful for sustained drug delivery systems.

Table 4. Fitting of the release data to the mathematical models for drug release kinetics. R^2 is the correlation coefficient.

PCL/CAM	Zero order	First order	Higuchi
95/5	$R^2 = 0.804$	$R^2 = 0.976$	$R^2 = 0.931$
80/20	$R^2 = 0.972$	$R^2 = 0.797$	$R^2 = 0.961$
40/60	$R^2 = 0.982$	$R^2 = 0.87$	$R^2 = 0.971$

3.3. Bacterial inhibition assay

The agar diffusion test was carried out on PCL/CAM 80/20 and 50/50 blends, which are characterized by a constant release rate according to the preceding section. Inhibition zones were observed when the released solutions containing CAM were placed on plates with a layer of *E. Coli* (see Fig. 7 and Table 5). PCL was used as negative control, and inhibition zones could not be detected from its leachates (Fig. 7a). A CAM solution of concentration 1 mg/mL (the solubility of CAM in water at 25 ºC is 2.5 mg/mL [31]) was used as positive control, resulting in inhibition zones of average radius of 0.8 cm (Fig. 7b). In case of the PCL/CAM blends, the concentration of CAM in the leachate at different times was calculated from the kinetic models obtained in the preceding section. In all cases, the entire drug was released from the polymer after 24 h, as confirmed also by ATR spectroscopy of the final films. After 24 h, the concentration of CAM in the leachate was 0.7 mg/mL for the PCL/CAM 80/20 sample, and 1.1 mg/mL for the PCL/CAM 50/50 blend. Overall, the inhibition radii are proportional to the concentration of CAM in the solutions, indicating that CAM can be released in a controlled way from its blends with PCL, without losing antibacterial activity. Moreover, it is also known that amorphous forms possess a higher apparent solubility in comparison to their crystalline counterparts [32, 33], and blending with PCL could be an interesting strategy to obtain therapeutical concentrations above the solubility limit of the drug.

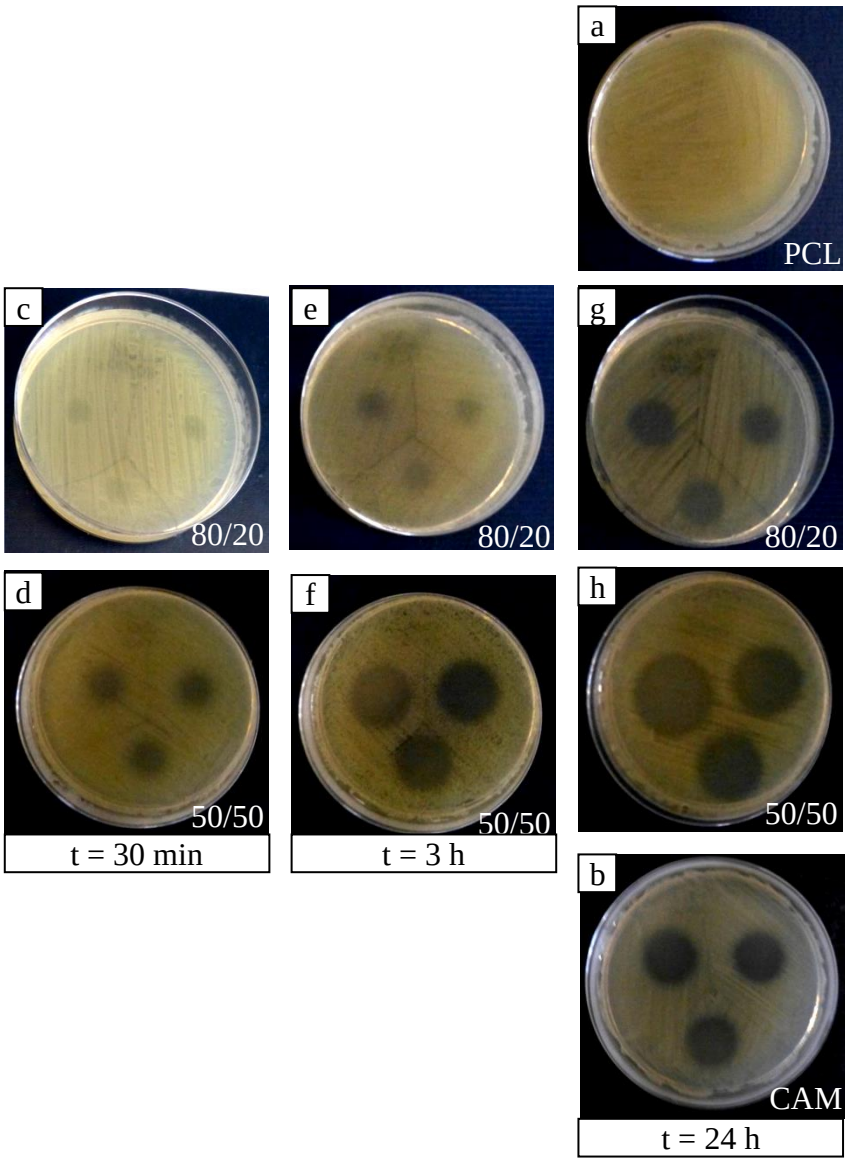

Fig.7. Images of inhibition zones created after pouring on LB agar plates with *E. Coli* 5 µl drops of the leachates obtained from (a) PCL after 24 h, (b) chloramphenicol solution of 1 mg/mL, (c) PCL/CAM 80/20 after 30 min, (d) PCL/CAM 50/50 after 30 min, (e) PCL/CAM 80/20 after 3 h, (f) PCL/CAM 50/50 after 3 h, (g) PCL/CAM 80/20 after 24 h, and (h) PCL/CAM 50/50 after 24 h.

Table 5. Average radius of the inhibition zones measured after fixed intervals, and the amount of drug released at each time.

Radius (cm)	30 min	3 h	24 h
CAM	0.8	0.8	0.8
PCL/CAM 80/20	0.4	0.5	0.8
PCL/CAM 50/50	0.5	1	1.3
% Drug released	20 %	60 %	100 %

4. Conclusions

Miscibility has been confirmed in the PCL/CAM system according to the intermediate glass transition temperature criterion. The analysis of the melting point depressions using the expression of Flory indicates negative interaction parameters for both PCL-rich and CAM-rich blends.

The analysis by FTIR spectroscopy of the PCL/CAM blends shows new bands in the C=O stretching region attributable to C=O···H-O interactions between the carbonyl groups of PCL and the hydroxyl groups of CAM. In addition, the OH stretching band of molten CAM is observed to shift to higher wavenumbers. These changes suggest the formation of new C=O···H-O interactions between PCL and CAM, mainly at the expense of the O-H···O-H interactions present in pure CAM, since reducing the number of hydroxyl-hydroxyl interactions reduces their degree of cooperativity and shifts the band to higher wavenumbers.

The analysis of the spherulitic morphology of the blends by AFM shows that the addition of CAM to PCL results in less defined spherulites, showing a laxer morphology, characteristic of miscible blends. The XRD analysis shows that the maximum CAM content in the blend to achieve an amorphous solid dispersion is about 10 wt% CAM. Release kinetic analyses show that CAM can be completely released from the PCL/CAM films in about 7 hours in aqueous media. First order kinetics are observed for the samples containing CAM in amorphous form, and zero order kinetics for samples containing crystalline CAM. Finally, the agar diffusion test against *E. Coli* (a gram-negative bacteria associated with biofilm formation on medical devices) shows that CAM can be released in a controlled way from its blends with PCL without losing antibacterial activity.

Acknowledgements

The authors are thankful for funds from the Spanish Ministry of Innovation and Competitiveness MINECO (MAT2016-78527-P), the Basque Government, Department of Education (IT-927-16) and the EU iPROMEDAI COST Action TD1305.

References

[1] Y. Kawabata, K. Wada, M. Nakatani, S. Yamada, S. Onoue, Formulation design for poorly water-soluble drugs based on biopharmaceutics, Int. J. Pharm. 420 (2011) 1-10.

[2] N. Shah, H. Sandhu, D.S. Choi, H. Chokshi, A. Malick, Amorphous Solid Dispersions. Theory and Practice, New York: Springer (2014).

[3] Y. Fu, W. Kao, Drug release kinetics and transport mechanisms of non-degradable and degradable polymeric delivery systems, Expert Opin Drug Deliv. 7(4) (2010) 429–444.

[4] N. Kamaly, B. Yameen, J. Wu, O. Farokhzad, Degradable controlled-release polymers and polymeric nanoparticles: mechanisms of controlling drug release, Chem Rev. 116(4) (2016) 2602–2663.

[5] M. Labet, W. Thielemans, Synthesis of polycaprolactone: a review, Chem. Soc. Rev. 38 (2009) 3484–3504.

[6] I. McLean, J. Schwab, A. Hillegas, A. Schlingman, Susceptibility of micro-organisms to chloramphenicol (chloromycetin), J Clin Invest. 28(5) (1949) 953–963.

[7] S. Kalita, B. Devi, R. Kandimalla, K.K. Sharma, A. Sharma, K. Kalita, A.C. Kataki, J. Kotoky, Chloramphenicol encapsulated in poly-e-caprolactone-pluronic composite: nanoparticles for treatment of MRSA-infected burn wounds, Int. J. Nanomedicine 10 (2015) 2971-2984.

[8] T. Vasconcelos, B. Sarmento, P. Costa, Solid dispersions as strategy to improve oral bioavailability of poor water soluble drugs, Drug Discovery Today 12(23-24) (2007) 1068-1075.

[9] K. H. Norris, C. Williams, Optimization of mathematical treatments of raw near-infrared signal in the measurement of protein in hard red spring wheat. i. influence of particle size, Cereal Chem. 61(2) (1984) 158–165.

[10] P. Cumpson, C. Clifford, J. Portoles, J. Johnstone, M. Munz, Cantilever spring-constant calibrationin atomic force microscopy, Nano Sci. Technol. 8 (2008) 289-314.

[11] J. S. Boateng, K. H. Matthews, A. D. Auffret, M. J. Humphrey, H. N. Stevens, G. M. Eccleston, In vitro drug release studies of polymeric freeze-dried wafers and solvent-cast films using paracetamol as a model soluble drug, Int. J. Pharm. 378 (2009) 66-72.

[12] T. Higuchi, Mechanism of sustained-action medication. Theoretical analysis of rate of release of solid drug dispersed in solid matrices, J. Pharm. Sci. 52(12) (1963) 1145-1149.

[13] S. Khan, H. Batchelor, Hanson, I.Y. Saleem, Y. Perrie, A.R. Mohammed, Dissolution rate enhancement, in vitro evaluation and investigation of drug release kinetics of chloramphenicol and sulphamethoxazole solid dispersions, Drug Develo Ind. Pharm. 39(5) (2013) 704-715.

[14] N. Hernandez-Montero, E. Meaurio, K. Elmiloudi, J.R. Sarasua, Novel miscible blends of poly(p-dioxanone) with poly(vinyl phenol), Eur. Polym. J. 48 (2012) 1455–1465.

[15] A. Lejardi, J.R. Sarasua, A. Etxeberria, E. Meaurio, Miscible blends of poly(ethylene oxide) with brush copolymers of poly(vinyl alcohol)-graft-poly(L-lactide), J. Polym. Sci. B 54 (2016) 1217–1226.

[16] E. Meaurio, E. Zuza, J.R. Sarasua, Miscibility and specific interactions in blends of poly(L-lactide) with poly(vinylphenol), Macromolecules 38(4) (2005) 1207-1215.

[17] T. G. Fox, Influence of diluent and of copolymer composition on the glass temperature of a polymer system, Bull. Am. Phys. Soc. 1 (1956) 123-132.

[18] J. Kerc, S. Srcic, Thermal analysis of glassy pharmaceuticals, Thermochim. Acta, 248 (1995) 81-95.

[19] E. Meaurio, N. Hernandez-Montero, E. Zuza, J.R. Sarasua, Miscible blends based on biodegradable polymers, Characterization of Polymer Blends: Miscibility, Morphology and Interfaces, 1, S. Thomas, Y. Grohens, Jyotishkuma, Edits., Weinheim, Wiley (2015) 7–92.

[20] J. Flory, Principles of Polymer Chemistry, New York: Cornell University Press (1953).

[21] L. M. Robenson, Polymer Blends. A comprehensive review, Hanser (2007).

[22] M. M. Knopp, L. Tajber, Y. Tian, N.E. Olesen, D.S. Jones, A. Kozyra, K. Löbmann, K. Paluch, C.M. Brennan, R. Holm, A.M. Healy, G. Andrews, T. Rades, Comparative study of different methods for the prediction of drug−polymer solubility, Mol. Pharm. 12 (2015) 3408−3419.

[23] D. Rohindra, Miscibility determination in poly(e-caprolactone)/poly(vinil formal) blend by equilibrium melting temperature and spherulite morphology, J. Macromol. Sci. B 48 (2009) 1103-1113.

[24] M. Al-Hussein, G. Strobl, The Melting Line, the Crystallization Line, and the Equilibrium Melting Temperature of Isotactic Polystyrene, Macromolecules 35 (2002) 1672–1676.

[25] L. Mandelkern, Crystallization of Polymers, 2 ed., 1, New York: Cambridge University Press (2002).

[26] E. Meaurio, E. Sanchez-Rexach, A. Butron, J. R. Sarasua, The Conformation of Chloramphenicol in the ordered and disorderd phases, J. Antibiotics (2018) submitted.

[27] D. Sajan, G. D. Sockalingum, M. Manfait, I. Hubert Joe, V.S. Jayakumar, NIR-FT Raman, FT-IR and surface-enhanced Raman scattering spectra, with theoretical simulations on chloramphenicol, J. Raman Spectrosc. 39 (2008) 1772-1783.

[28] J. Jingou, H. Shilei, L. Weiqi, W. Danjun, W. Tengfei, X. Yi, Preparation, characterization of hydrophilic and hydrophobic drug in combine loaded chitosan/cyclodextrin nanoparticles and in vitro release study, Colloids Surf. B 83 (2011) 103–107.

[29] C. Hou, T. Yang, X. Sun, Z. Ren, H. Li, S. Yan, Branched crystalline patterns of poly(e-caprolactone) and poly(4-hydroxystyrene) blends thin films, J. Phys. Chem. B 120 (2016) 222-230.

[30] J. Siepmann, N.A. Peppas, Modeling of drug release from delivery systems based on hydroxypropyl methylcellulose (HPMC), Adv. Drug Deliv. Rev. 48 (2001) 139-157.

[31] D. Szulczewski, F. Eng, Chloramphenicol, Analytical Profiles of Drug Substances, K. Florey, Ed., Academic Press (1975) 47-90.

[32] S.B. Teja, S. Patil, G. Shete, S. Patel, A.K. Bansal, Drug-excipient behavior in polymeric amorphous solid dispersions., J. Excipients Food Chem. 4(3) (2013) 70-94.

[33] B.C. Hancock, M. Parks, What is the true solubility advantage for amorphous pharmaceuticals?, Pharm. Res. 17(4) (2000) 397-404.

Supporting Information

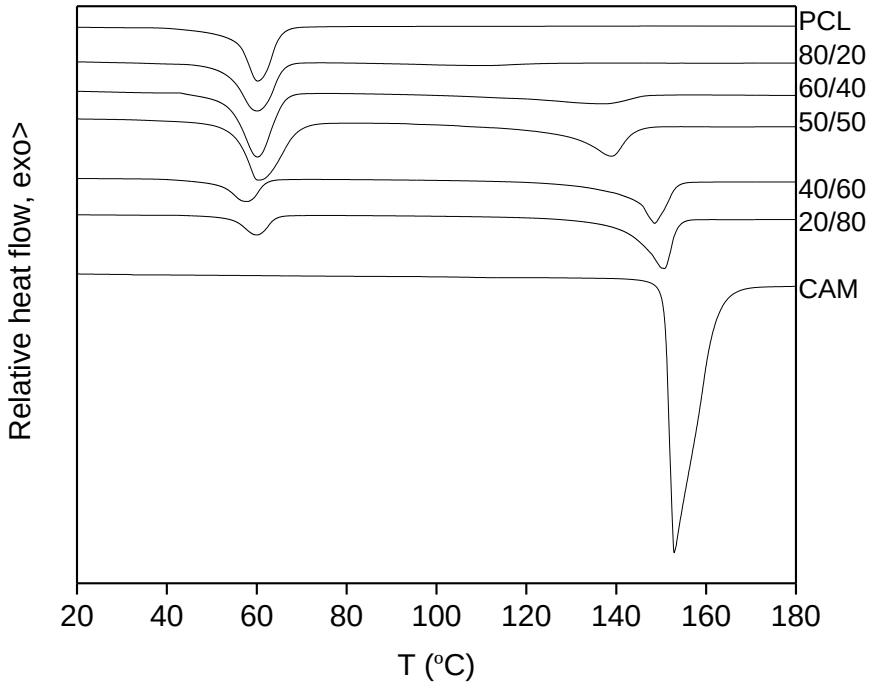

Figure S1. First scan DSC traces for PCL, CAM and PCL/CAM blends.

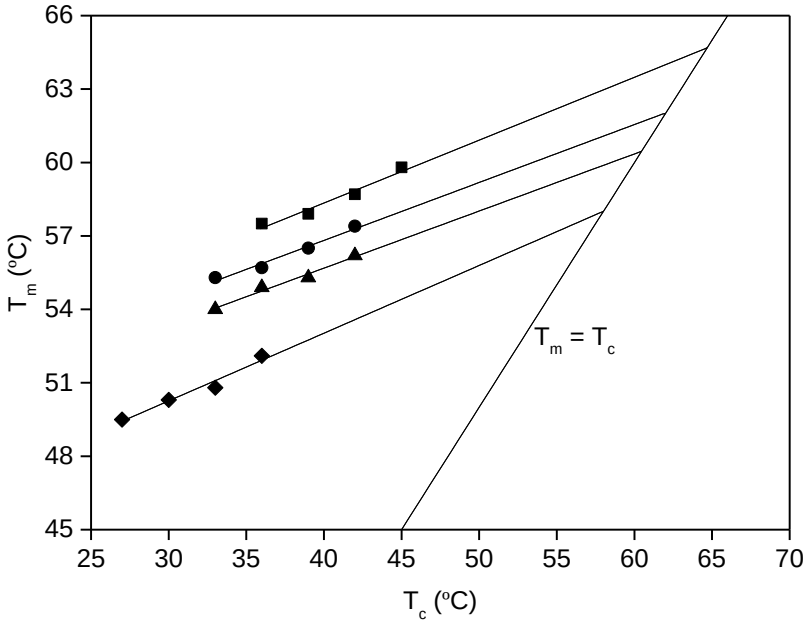

Figure S2. Hoffman-Weeks extrapolations for (■) PCL, (●) PCL/CAM 90/10, (▲) PCL/CAM 85/15, and (♦) PCL/CAM 80/20.

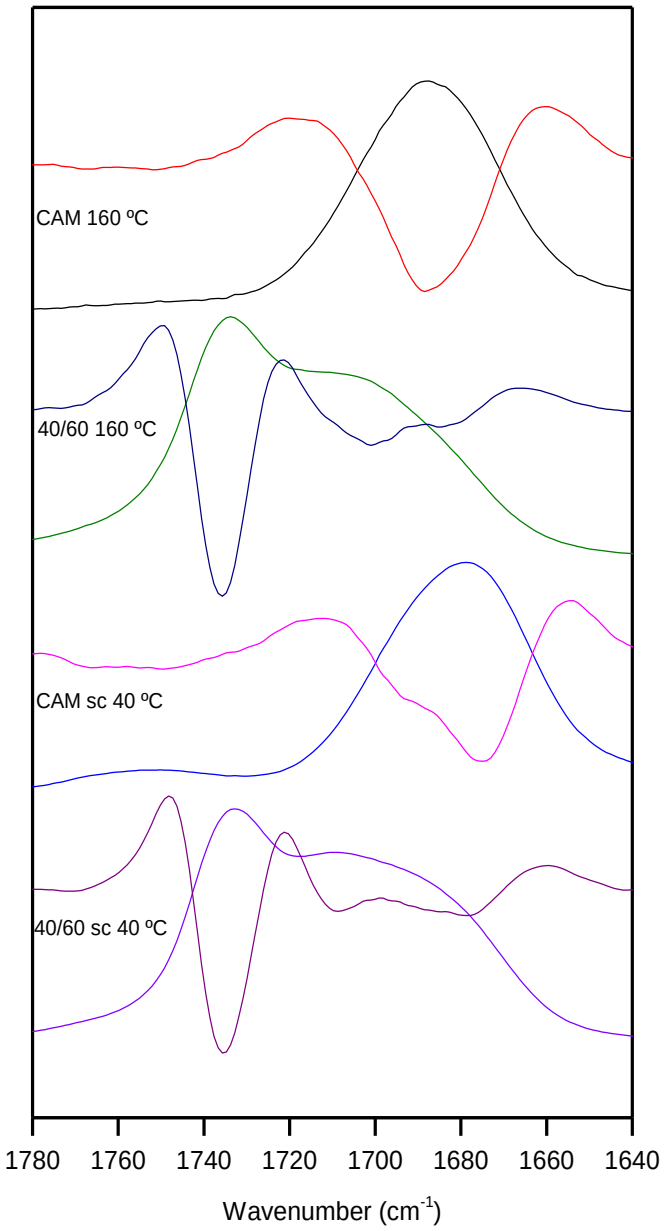

Figure S3. Spectra and Norris second derivatives for CAM and for the PCL/CAM 40/60 blend in both molten (160 ºC) and supercooled samples (40 ºC).